Modeling and analysis of actively Q-switched Fe: ZnSe laser pumped by a 2.8 μm fiber laser*

LIANG Xiaolin, ZHOU Songqing, LIU Zhizhuang, and BAO Bengang**

College of Intelligent Manufacturing, Hunan University of Science and Engineering, Yongzhou 425199, China

(Received 9 February 2023; Revised 22 March 2023)

A theoretical model concerning active Q-switching of an Fe: ZnSe laser pumped by a continuous-wave (CW) 2.8 μm fiber laser is developed. Calculations are compared with the recently reported experiment results, and good agreement is achieved. Effects of principal parameters, including pump power, output reflectivity, ion concentration and temperature of crystal, on the laser output performance are investigated and analyzed. Numerical results demonstrate that similar to highly efficient CW Fe: ZnSe laser, low temperature of the crystal is significant to obtain high peak power Q-switched pulses. The numerical simulation results are useful for optimizing the design of actively Q-switched Fe: ZnSe laser.

Document code: A **Article ID:** 1673-1905(2023)09-0513-6

DOI https://doi.org/10.1007/s11801-023-3016-y

Mid-infrared lasers have attracted much attention for their potential applications in laser surgery, spectroscopy[1-4], infrared countermeasures, laser communication, and environmental monitoring, etc. Specifically, lots of molecular absorption lines lie in the 3—5 μm wavelength region which overlaps with the transparency window of atmosphere. There are several approaches to achieve lasing in the 3—5 μm band including gas lasers[5,6], semiconductor lasers[7], fiber lasers[8] and solid-state lasers[9-15]. The gas lasers are mainly the direct-current (DC) discharge-driven continuous-wave (CW) HF/DF chemical laser and the non-chain pulsed discharge HF/DF laser[5,6]. The semiconductor lasers involve quantum cascade lasers[7], the development of which is very rapid during the past decade. The solid-state lasers include optical parametric oscillators (typically using periodically poled lithium niobate (PPLN) and $ZnGeP_2$ (ZGP) crystals as nonlinear media) and the transition metal iron doped ZnSe/ZnS (Fe: ZnSe or Fe: ZnS) lasers[9-13]. Compared with the lasers mentioned above, the Fe: ZnSe or Fe: ZnS lasers, which are an innovative solid state lasers in the mid-infrared range of 4—5 μm, have the advantages of high efficiency, excellent beam quality, wide wavelength-tuning range and compact structure of optical cavity[14,15], etc. Therefore, Fe: ZnSe/Fe: ZnS lasers have become one of the hottest research topics, and lots of efforts have been paid for their development in recent years.

Due to the broad absorption band (2.6—3.4 μm) of Fe: ZnSe/Fe: ZnS crystals, various pump sources were employed to excited the crystals, for instance, high power solid-state Er: YAG/Er: Cr: YSGG/Er: YAP lasers[14,16,17], high power Cr: ZnSe lasers and Cr: Yb: Ho: YSGG lasers[18], high energy non-chain pulsed HF lasers[19], and high energy optical parametric oscillators[20]. Aside from these oscillators, Fe: ZnSe crystal is widely used for power amplification at 4 μm in master oscillator power amplifier (MOPA) regime. POTEMKIN et al[21] demonstrated a sub-terawatt mid-infrared femtosecond hybrid laser with an output energy of ~6 mJ and a pulse width of ~200 fs based on a multipass Fe: ZnSe amplifier pumped by a YSGG: Cr: Er laser in 2016. MARTYSHKIN et al[22] reported an Fe: ZnSe MOPA system seeded by a room temperature (RT) gain-switched Fe: ZnSe laser with a maximum pulse energy of 60 mJ and wavelength tuning range of 3.8—5.0 μm in 2021. Generally, all the demonstrations above employed solid-state lasers for pumping. As known to all, fiber lasers possess several impressive advantages, including outstanding beam quality, good stability and high brightness[23], which are very suitable as pumping sources. Thanks to the powerful laser diode and increasingly mature manufacture of fluoride fiber, mid-infrared fiber lasers at 3 μm have been developed rapidly in the past decades, of which the highest output power was as high as 65 W. As such, several Fe: ZnSe lasers have been demonstrated by employing a mid-infrared fiber laser as the pump source recently. In 2018, PUSHKIN et al[24] demonstrated a compact, highly efficient CW Fe: ZnSe pumped by an Er: ZBLAN fiber laser with an

* This work has been supported by the 2021 Annual Instructional Science and Technology Program of Yongzhou (No.2021YZKJ09), and the Science Research Project of Hunan Institute of Science and Technology (No.21xky040).

** E-mail: 122322855@qq.com

output power of 2.1 W and a slope efficiency as high as 59% by liquid nitrogen cooling. Besides the foreign CW Fe: ZnSe lasers, in 2023, SHEN et al[25] presented the first domestic demonstration of a watt-level CW Fe: ZnSe laser with a central wavelength at 3.8 μm. For Q-switched operation, UEHARA et al[26] reported an acousto-optically Q-switched Fe: ZnSe laser pumped by a CW fluoride fiber laser in 2020. Stable Q-switched pulses with a pulse duration of ~20 ns and a repetition rate of 40 kHz at 4 μm were achieved, of which the maximum peak power was as high as 1.1 kW.

Compared with the experimental demonstrations, the demonstrations of theoretical study were much less. In 2018, PAN et al[27] reported a theoretical model of a CW Fe: ZnSe laser, and the output characteristics of the laser was simulated, in which only two energy levels' populations were taken into consideration. Nevertheless, the model of Q-switched Fe: ZnSe laser is much different from the CW regime, and no theoretical study about a Q-switched Fe: ZnSe laser has been demonstrated up to date.

In this paper, a theoretical model of an actively Q-switched Fe: ZnSe laser pumped by a CW 2.8 μm fiber laser is established based on the rate equations theory and simulated by the finite difference method. Our aim here is to theoretically investigate the characteristics of the actively Q-switched Fe: ZnSe laser for optimizing further relevant experiments. Effects of the pump power, output reflectivity, iron concentration and temperature of Fe: ZnSe crystal on the output performance of the actively Q-switched laser, including the repetition rate, pulse duration and peak power, are investigated and analyzed. The simulated pulse width and output power of the actively Q-switched Fe: ZnSe laser are consistent with the experimental results reported by UEHARA. The simulation results show that the output reflectivity of 0.7—0.8, a relatively higher iron-doped concentration, and low temperature of the crystal are crucial to obtain high quality Q-switched pulses. And the results could be used as a guide for optimizing the principal parameters of an actively Q-switched Fe: ZnSe laser.

We consider a typical actively Q-switched Fe: ZnSe laser with a linear cavity, which is analogous to the laser system in Ref.[26], as schematically shown in Fig.1. The pump beam from the CW 2.8 μm fiber laser is collimated and then coupled into the gain medium, i.e., the Fe: ZnSe crystal through a coupling system consisted of two CaF_2 lenses. The cavity was formed by two plano-concave mirrors with a radius of curvature of 100 mm. The left one, namely, the feedback mirror, was coated with a high reflection of ~99% at 3.9—4.8 μm and a high transmittance of >99.5% at 2.7—3.4 μm. While the output mirror was coated with a high reflection ~99% at 2.7—3.4 μm and a partial reflection (to be optimized in this model) at 3.9—4.8 μm. The Fe: ZnSe crystal was wrapped with a piece of indium foil and mounted into a copper heat sink. The temperature of the crystal, which is controlled by a cryostat, would be tuned continuously from 77 K to 300 K. The Q-switch inserted in the cavity is used to modulate the loss of the cavity at a specified repetition rate. There are few Q-switches in the mid-infrared 4 μm band, mainly including acousto-optical switch and mechanical switch, both of which the repetition rate ranges are typically 10—50 kHz and 0.1—10 kHz, respectively.

The simplified energy levels and related energy transition processes of this laser system are shown in Fig.2. The Fe^{2+} ions at the ground state $^5E|g\rangle$ are excited to the first excited state $^5T_2|3\rangle$ via ground-state absorption (GSA), and then relax to the upper laser level $^5T_2|2\rangle$ rapidly. The transition $^5T_2|2\rangle \rightarrow {}^5E|1\rangle$ produces emission of 4 μm waveband. The temperature interferes remarkably with the lifetime of $^5T_2|2\rangle$, which is around 57 μs at low temperature (LT) of 77 K and down dramatically to ~370 ns at RT of ~300 K[28]. The Fe^{2+} ions at the upper laser level $^5T_2|2\rangle$ jump to the $^5T_2|4\rangle$ level by the excited-state absorption (ESA) at 4 μm, which depopulates the particle density of upper laser level. However, prompt decay from $^5T_2|4\rangle$ to $^5T_2|2\rangle$ in turn increases the inversion of population for lasing at 4 μm[27]. The particle population densities from ground state to related upper excited states are labeled as N_0, N_1,…, N_4, respectively.

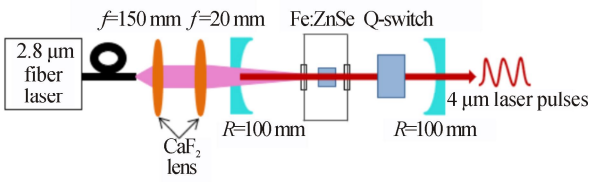

Fig.1 Schematic layout of the active Q-switching of an Fe: ZnSe laser pumped by a CW 2.8 μm fiber laser

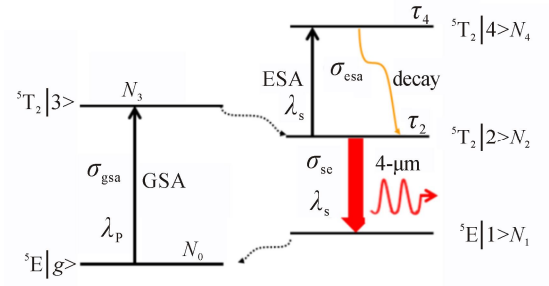

Fig.2 Schematic diagram of simplified Fe^{2+} ion energy-levels, indicating the lasing process relevant to the transition of $^5T_2|2\rangle$->$^5E|1\rangle$ (GSA: ground-state absorption; ESA: excited-state absorption)

According to the energy levels and associated processes shown in Fig.2, the rate equations for the population densities N_i of the Fe: ZnSe laser system and photon density can be respectively given by

$$\frac{\mathrm{d}\phi}{\mathrm{d}t}=\frac{c\phi}{2L}[\sigma_{se}N_2(z,t)l+0.5\ln(R_1R_2)-\alpha l-\delta]+\frac{N_2(z)}{\tau_2}, \quad (1)$$

$$\frac{\mathrm{d}N_2}{\mathrm{d}t}=\frac{\sigma_{gsa}\lambda_p P_p}{hcA_p}N_0-\sigma_{se}\phi cN_2-\sigma_{esa}\phi cN_2-\frac{N_2}{\tau_2}+\frac{N_4}{\tau_4}, \quad (2)$$

$$\frac{dN_4}{dt} = c\sigma_{esa}\phi N_2 - \frac{N_4}{\tau_4}, \tag{3}$$

$$N_t = N_0(z) + N_2(z) + N_4(z), \tag{4}$$

where ϕ is the photon density inside of the cavity, h is the Planck's constant, c is the velocity of light in vacuum, and τ_i is the lifetime of energy level i. α and l are the intrinsical loss and the length of the crystal. λ_p and λ_L are the wavelengths of pump and laser signals, i.e., 2.8 μm and 4.1 μm in this model, respectively. σ_{gsa} and σ_{esa} are the ground-state absorption cross-section and the excited-state absorption cross-section of the Fe: ZnSe crystal at 2.8 μm and 4.1 μm, respectively. σ_{se} is the emission cross section of the laser transition from $^5T_2|2>$ to $^5E|1>$ at 4.1 μm. P_p is the pump power, and N_t is the dopant concentration. R_1 and R_2 are the reflectivity of the feedback and the output coupler, respectively. L is the optical length of the cavity. δ is the modulation loss in the cavity, which is assumed to be a simple on-and-off pulse profile, i.e., squared waveform. The latest two parameters could be expressed by Eq.(5) and Eq.(6). The output average power of the laser could be expressed by the following equation[29]

$$L = nl + l_{air}, \tag{5}$$

$$\delta = \begin{cases} \delta_0 & (0 < t \le kT) \\ 0 & (kT < t \le T) \end{cases}, \tag{6}$$

$$P_{out} = 0.5c\phi\frac{hc}{\lambda_L}\pi r_s^2(1-R_2), \tag{7}$$

where n is the index of refraction of the crystal, and l_{air} is the length of cavity in air. T is the modulation period of the active Q-switch, k is the duty-cycle of modulation of the Q-switch, and δ_0 is a constant. r_s is the radius of laser beam.

In our modeling, considering the relatively low power in the active fiber and thus ignoring the nonlinear effects, numerical calculations are carried out with the parameters listed in Tab.1.

Firstly, typical dynamic population density of main levels and photons are investigated under conditions of 2.6 W pump power, 80% output reflectivity, and a dopant concentration of 3.5×10^{18} cm^{-3} in forward pump scheme. The repetition rate of the Q-switch is set to be 10 kHz. The calculated pulse train and profile of an individual pulse at 10 kHz in steady state are shown in Fig.3. The initial values of N_2 and N_4 are all set to be near zero. Generally, the Q-switched pulse generation contains two stages. At the first stage, the Q-switch is off, correspondingly, the loss in the cavity is very high, which prevent the oscillating. During the stage, the particles of upper laser level N_2 accumulate continuously, and the photon in the cavity is rather few. The particles of N_4 stay around zero as well. When the Q-switch is turned on, the state of the laser shifts to the second stage, in which the oscillation is established. As a consequence, significant amplification of photon creates a huge pulse, accompanied with depopulation of upper laser level particles. The amplitude the actively Q-switched pulse train is rather stable and the pulse had a typical Gaussian shape. It should be pointed out that the population normalization is performed with respect to the total doping concentration, while the lasing intensity is normalized in comparison with the maximal photon density. During this stage, the population of N_4 increases slightly due to the short lifetime of $^5T_2$ |4> which results in a fast relaxation to $^5T_2|2>$. The laser pulse width is calculated to be around 35 ns in this case.

Tab.1 Parameters used in the simulation

Parameter	Value	Parameter	Value
Pump wavelength λ_p	2.8 μm	Pump beam waist ω_p	230 μm
Laser wavelength λ_s	4.1 μm	Laser beam waist ω_s	210 μm
Absorption cross-section σ_{gsa}	0.87×10^{-18} cm^{-2} at 77 K[2] 0.7×10^{-18} cm^{-2} at 300 K[11]	Radiative emission lifetime of upper level τ_2	57 μs at 77 K[28] 0.37 μs at 300 K[28]
Emission cross-section σ_{se}	1.1×10^{-18} cm^{-2} at 77 K[2] 2.1×10^{-18} cm^{-2} at 300 K[15]	Ion concentration N_t	(1, 3.5, 5, 8)$\times10^{18}$ cm^3
Intrinsic loss α	0.1 cm^{-1}[27]	Length of crystal l	8 mm
Normalized ESA strength σ_{esa}/σ_{se}	0.17[27]	Lifetime of $^5T_2$ |3>level τ_3	~1 μs
Reflectivity of output R_1	0.99	Reflectivity of output R_2	TBD[a]
Duty-cycle k	10%	Refractive index n	2.4

a: to be determined

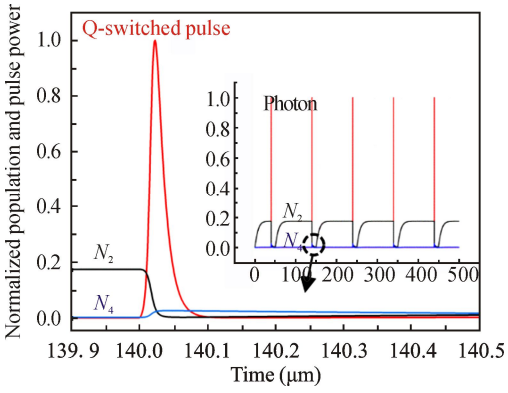

Fig.3 Density evolution of photon and energy levels of N_2 and N_4 (Inset shows their variations and correlations on a large scale)

The pulse width and peak power of the actively Q-switched Fe: ZnSe laser is investigated with an output reflectivity (R_2) of 0.75 by varying the pump power, as

shown in Fig.4. The pulse width decreases, while the pulse peak power increases with the pump power, respectively. The trends of these two parameters are consistent with those experimental results in Ref.[30]. Theoretically, with the increase of the pump power, the pump rate becomes higher, and thus the cavity needs less time to generate a laser pulse, resulting in a shorter pulse width. As for the peak power, the average output power is promoted with pump power before the gain gets saturated. Correspondingly, the pulse energy increases when the repetition rate is fixed. Therefore, the peak power is improved due to the combination of higher pulse energy and shorter pulse width.

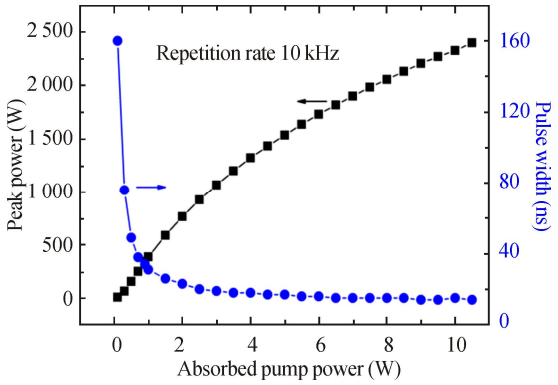

Fig.4 The peak power and pulse width as a function of absorbed pump power

Output reflectivity is another key factor that affects the performance of many ions-doped solid-state lasers. The output reflectivity refers to the ratio of the energy inside and outside the cavity. The output characteristics of the actively Q-switched laser pulses are simulated by varying the reflectivity of the output mirror, as shown in Fig.5. The peak power and the average power increase initially and then fall, both of which are peaked at the reflectivity range of 0.7—0.8. For pulse width, it has an inverse trend, that is, the pulse width reaches a minimum value at the reflectivity of ~0.7. Hence, the output coupling ratio is supposed to be designed at ~0.3 if higher peak power and shorter pulse are needed. The peak power related to output reflectivity could be expressed and explained by Eq.(8). The peak power is inversely proportional to the reflectivity, however, with higher output reflectivity, the threshold of inverse population Δn_t decreases. Therefore, the part in the second brackets of Eq.(8) is proportional to the reflectivity indirectly. As such, the optimal reflectivity of output mirror should be chosen to be 0.7—0.8 for shorter pulse width and higher peak power laser pulses.

$$P_{\text{peak}} \propto (1-R)\left(\Delta n_i - \Delta n_t \ln\frac{\Delta n_i}{\Delta n_t} - \Delta n_t\right). \tag{8}$$

Fig.6 presents the output of laser pulses with different concentrations of iron doped ZnSe crystals under a pump power of 2.6 W and an output reflectivity of 0.7. The peak power and the average power increased almost synchronously with the increment of ion concentration, while the pulse width decreases. Before the gain saturation occurring, the higher the ion concentration, the more particles participating laser pulse generation. Nevertheless, it is not a wise choice to continuously increase the concentration, because the interaction between ions will be enhanced in higher concentration, which would in turn induce quenching and lowering the output power. As a result, considering the interaction effect between ions and length of crystal, using a relatively high concentration dopant crystal is beneficial to obtaining high power laser pulses[27].

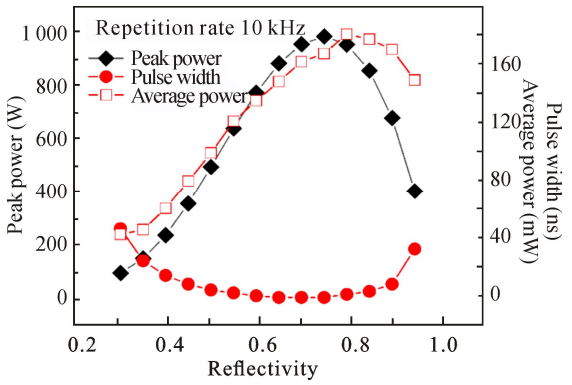

Fig.5 The peak power, pulse width and average power versus output reflectivity

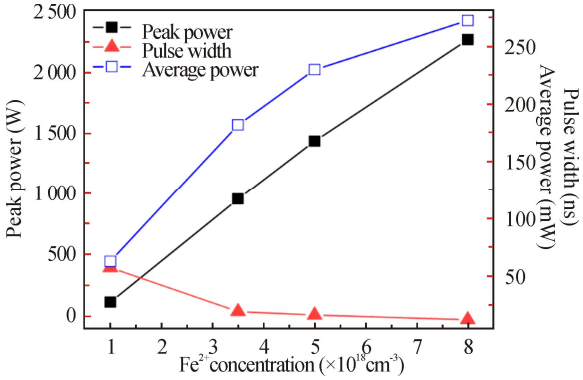

Fig.6 The influence of Fe^{2+} concentration on the output characteristics

As stated before, the temperature of Fe: ZnSe crystal plays a very important role in the lifetime of upper laser level, which affects the laser output significantly. The higher the temperature of the crystal is, the shorter the lifetime of the upper laser level $^5T_2|2>$. That is, the lifetime is as long as 57 μs at 77 K, and lowered to around 42 μs at a higher temperature of 180 K, then down to dramatically to ~370 ns at 300 K. The output behaviors as a function of pump power are compared under three typical temperatures of the crystal, ignoring the heat load caused by pump power, as shown in Fig.7. The concentration and output reflectivity are 3.5×10^{18} cm^{-3} and 0.7, respectively. Interestingly, it is hard to achieve a CW

output of Fe: ZnSe laser at a temperature above 250 K, whereas it seems to be feasible to obtain an actively Q-switched operation at RT of 300 K. However, the discrepancy in the average power, pulse width and peak power at different temperatures is fairly significant. Fig.7(a) gives the variation of pulse width and peak power. It is common that the pulse width drops off rapidly and then decrease slowly for all temperatures as increasing the pump power. While the peak power is linear with pump power. In the pump power range of 0.3—4.8 W, the pulse width of the actively Q-switched laser pulse is shortened from ~130 ns to ~15 ns accompanied with the peak power of up to 1.6 kW at LT of 77 K. The minimum pulse widths at the maximum pump power of 4.8 W are 15 ns, 28 ns and 53 ns at the corresponding temperatures of 77 K, 180 K, and 300 K, respectively. The shortest pulse width and the highest peak power are a factor of 3 greater and nearly one order of magnitude smaller at RT of 300 K. The difference in pulse width and peak power of laser pulse could be explained as follows. For a certain pump power, the longer the lifetime, the easier to obtain the reverse population. As such, it takes shorter time and needs lower pump rate to establish the oscillation in the cavity to create a laser pulse. From Fig.7(b), one could find that the optical conversion efficiency of this laser system at LT is much higher than RT. Therefore, for obtaining more powerful laser pulses, the crystal should be cooled to LT, for instance, using liquid nitrogen to 77 K in a cryostat. Indeed, the introduction of the cryostat brings inconvenience and promotes the cost of the laser system. Recently, there is a demonstration using a thermoelectric cooler (TC) to cool the crystal to 190 K[31], which is relatively compact and economic. Consequently, cooling the crystal with a TC is an acceptable compromise.

The modeling and simulations above can be used for optimizing actively Q-switched Fe: ZnSe lasers. For example, if laser pulses with high peak power and narrow pulse width are desired, the combination of a relative high pump, an optimal reflectivity of the output mirror, a relatively high concentration dopant for gain medium selection, and low temperature of Fe: ZnSe crystal for working condition might be a good choice.

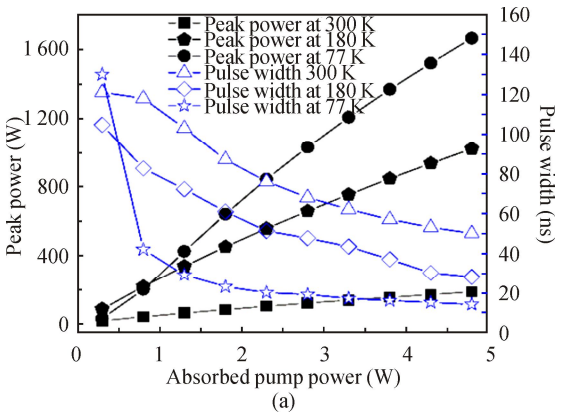

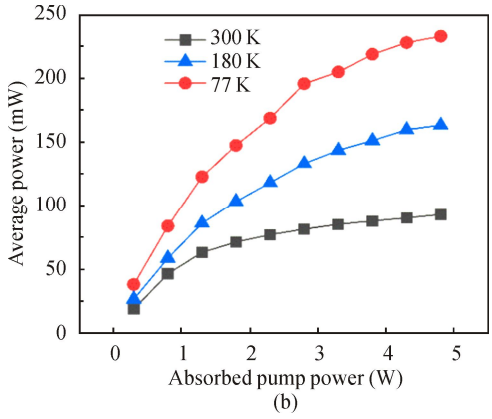

Fig.7 (a) Pulse width and peak power and (b) average power as a function of absorbed pump power at various temperatures

In conclusion, a theoretical model of an actively Q-switched, a 2.8 μm fiber laser pumped Fe: ZnSe laser based on rate equations is established to analyze the operation behaviors and output characteristics. Investigation of some important laser parameters, including pump power, reflectivity, etc, is carried out. Unlike CW output in low temperature, i.e., below 250 K, the actively Q-switched Fe: ZnSe laser could operate at RT. However, cooling the crystal to 77 K is necessary for obtaining more powerful laser pulses. The model and simulating results could provide the guide for design and optimization of an actively Q-switched Fe: ZnSe laser at 4 μm wavelength region.

Ethics declarations

Conflicts of interest

The authors declare no conflict of interest.

References

[1] JACKSON S D. Towards high-power mid-infrared emission from a fiber laser[J]. Nature photonics, 2012, 6(7): 423-431.

[2] MIROV S B, FEDOROV V V, MARTYSHKIN D, et al. Progress in mid-IR lasers based on Cr and Fe-doped II-VI chalcogenides[J]. IEEE journal of selected topics in quantum electronics, 2014, 21(1): 292-310.

[3] ZHU X, PEYGHAMBARIAN N. High-power ZBLAN glass fiber lasers: review and prospect[J]. Advances in optoelectronics, 2010, 1-23.

[4] AKIMOV V A, VORONOV A A, KOZLOVSKII V I, et al. Efficient IR Fe: ZnSe laser continuously tunable in the spectral range from 3.77 to 4.40 μm[J]. Quantum electronics, 2004, 34(10): 912.

[5] BASHKIN A S, GUROV L V, KURDYUKOV M V. Possibilities of improving the performance of an autonomous CW chemical DF laser by replacing the slot nozzles by the ramp ones in the nozzle array[J]. Quantum electronics, 2011, 41(8): 697-702.

[6] PAN Q, XIE J, WANG C, et al. Non-chain pulsed DF laser with an average power of the order of 100 W[J].

Applied physics B, 2016, 122(7)：1-6.

[7] BECK M, HOFSTETER D, AELLEN T, et al. Continuous wave operation of a mid-infrared semiconductor laser at room temperature[J]. Science, 2002, 295(11)：301-305.

[8] MAES F, FORTIN V, POULAIN S, et al. Room-temperature fiber laser at 3.92 μm[J]. Optica, 2018, 5(7)：761-764.

[9] XING T, WANG L, HU S, et al. Widely tunable and narrow-bandwidth pulsed mid-IR PP MgLN-OPO by self-seeding dual etalon-coupled cavities[J]. Optics express, 2017, 25(25)：31810-31815.

[10] QIAN C P, YAO B Q, ZHAO B R, et al. High repetition rate 102 W middle infrared $ZnGeP_2$ master oscillator power amplifier system with thermal lens compensation[J]. Opticsletters, 2019, 44(3)：715-718.

[11] ADAMS J J, BIBEAU C, PAGE R H, et al. 4.0–4.5-μm lasing of Fe: ZnSe below 180K, a new mid-infrared laser material[J]. Optics letters, 1999, 24(23)：1720-1722.

[12] EVANS J W, BERRY P A, SCHEPLER K L. 840 mW continuous-wave Fe: ZnSe laser operating at 4140 nm[J]. Optics letters, 2012, 37(23)：5021-5023.

[13] FROLOV M P, KOROSTELIN Y V, KOZLOVSKY V I, et al. 3 J pulsed Fe: ZnS laser tunable from 3.44 to 4.19 μm[J]. Laser physics letters, 2015, 12(5)：055001.

[14] FEDOROV V, MARTYSHKIN D, KARKI K, et al. Q-switched and gain-switched Fe: ZnSe lasers tunable over 3.60–5.15 μm[J]. Optics express, 2019, 27(10)：13934-13941.

[15] KERNAL J, FEDOROV V V, GALLIAN A, et al. 3.9–4.8 μm gain-switched lasing of Fe: ZnSe at room temperature[J]. Optics express, 2005, 13(26)：10608-10615.

[16] MYOUNG N S, MARTYSHKIN D V, FEDOROV V V, et al. Energy scaling of 4.3 μm room temperature Fe: ZnSe laser[J]. Optics letters, 2011, 36(1)：94-96.

[17] LI E, UEHARA H, YAO W, et al. High-efficiency continuous wave Fe: ZnSe mid-IR laser end pumped by an Er: YAP laser[J]. Optics express, 2021, 29(26)：44118-44128.

[18] ANTONOV V A, BUKIN V V, DOLMATOV T V, et al. Single-nanosecond-pulse lasing in heavily doped Fe: ZnSe[J]. IEEE photonics journal, 2021, 13(1)：150087.

[19] FIRSOV K N, GAVRISHCHUK E M, IKONNIKOV V B, et al. High-energy room-temperature Fe^{2+}: ZnS laser[J]. Laser physics letters, 2016, 13：015001.

[20] LI Y Y, YANG K, LIU G Y, et al. A 1 kHz Fe: ZnSe laser gain-switched by a $ZnGeP_2$ optical parametric oscillator at 77 K[J]. Chinese physics letters, 2019, 36(7)：074201.

[21] POTEMKIN F, BRAVY B, KOZLOVSKY V, et al. Toward a sub-terawatt mid-IR (4-5 μm) femtosecond hybrid laser system based on parametric seed pulse generation and amplification in Fe^{2+}: ZnSe[J]. Laser physics letters, 2016, 13：015401.

[22] MARTYSHKIN D, KARKI K, FEDOROV V, et al. Room temperature, nanosecond, 60 mJ/pulse Fe: ZnSe master oscillator power amplifier system operating at 3.8-5.0 μm[J]. Optics express, 2021, 29(2)：2387-2393.

[23] ZHU X, JAIN R. Numerical analysis and experimental results of high power Er/Pr: ZBLAN 2.7 μm fiber lasers with different pumping designs[J]. Applied optics, 2006, 45：7118-7125.

[24] PUSHKIN A V, MIGAL E A, UEHARA H, et al. Compact, highly efficient, 2.1-W continuous-wave mid-infrared Fe: ZnSe coherent source, pumped by an Er: ZBLAN fiber laser[J]. Optics letters, 2018, 43(24)：5941-5944.

[25] SHEN Y, WAN Y, WANG Y, et al. 3.8 μm continuous-wave all solid-state Fe: ZnSe laser[J]. Chinese journal of lasers, 2023, 50(14)：1401005. (in Chinese)

[26] UEHARA H, TSUNAI T, HAN B, et al. 40 kHz, 20 ns acousto-optically Q-switched 4 μm Fe: ZnSe laser pumped by a fluoride fiber laser[J]. Optics letters, 2020, 45(10)：2788-2791.

[27] PAN Q, CHEN F, XIE J, et al. Theoretical study of the characteristics of a continuous wave iron-doped ZnSe laser[J]. Laser physics, 2018, 28(3)：035002.

[28] FEDOROV V V, MIROV S B, GALLIAN A, et al. 3.77-5.05 μm tunable solid-state lasers based on Fe^{2+}-doped ZnSe crystals operating at low and room temperatures[J]. IEEE journal ofquantumelectronics, 2006, 42(9)：907-917.

[29] JACKSON S D, KING T A, POLLNAU M. Modelling of high-power diode-pumped erbium 3 μm fibre lasers[J]. Journal of modern optics, 2000, 47(11)：1987-1994.

[30] SHEN Y, WANG Y, LUAN K, et al. High peak power actively Q-switched mid-infrared fiber lasers at 3 μm[J]. Applied physics B：lasers and optics, 2017, 123(105)：1-6.

[31] FROLOV M P, KOROSTELIN Y V, KOZLOVSKY V I, et al. High-energy thermoelectric cooled Fe: ZnSe laser tunable over 3.75-4.82μm[J]. Optics letters, 2018, 43(3)：623-626.